Electronic structure and Fermi surface of PrMIn$_5$ (M=Co, Rh, and Ir) compounds

S. Elgazzar,[1,2,*] I. Opahle,[2] Manuel Richter,[2] and P. M. Oppeneer[3]
[1]*Department of Physics, Faculty of Science, Menoufia University, Shebin El-kom, Egypt*
[2]*IFW Dresden, P.O. Box 270016, D-01171 Dresden, Germany*
[3]*Department of Physics, Uppsala University, Box 530, S-751 21 Uppsala, Sweden*
(Received 6 September 2007; revised manuscript received 1 February 2008; published 7 March 2008)

We report density functional calculations of the electronic structure, Fermi surface, and de Haas–van Alphen (dHvA) quantities of the PrMIn$_5$ (M=Co, Rh, and Ir) compounds. Our investigation is carried out within the framework of the local density approximation, using a relativistic, full-potential band-structure method. A critical analysis of the electronic structures and the de Haas–van Alphen quantities is performed, which shows that good agreement with recent measurements is obtained when we assume the Pr 4f states to be localized. The topology of the Fermi surface is calculated to be similar to that of non-4f reference compounds, e.g., LaRhIn$_5$. The similarities of the Fermi surfaces and the dHvA extremal orbits among the compounds in the series are discussed. We, furthermore, compare our calculated effective masses with experimental measurements and discuss the differences between them.

DOI: 10.1103/PhysRevB.77.125105 PACS number(s): 78.20.−e, 71.20.−b, 71.28.+d

I. INTRODUCTION

Among the lanthanide compounds, praseodymium-based compounds have recently entered into the focus of scientific attention. Initially, heavy fermion (HF) behavior—sometimes combined with superconductivity—has been observed for a number of Ce, U, and Yb compounds (see, e.g., Refs. 1–3). Many of these compounds have been intensively investigated for years. More recently, the first observation of heavy fermion superconductivity was reported for the Pr skutterudite $PrOs_4Sb_{12}$.[4] Other Pr skutterudites, such as $PrFe_4P_{12}$, were recently discovered[5] to be heavy fermion materials with an enormously enhanced effective mass of 81 m_0. Particularly, the HF superconducting state in $PrOs_4Sb_{12}$ is drawing considerable attention,[6–9] as it appears to be of an unconventional type, possibly due to Cooper pairing mediated by quadrupolar fluctuations.[10]

Prior to the discovery of the heavy fermion Pr skutterudites, several other praseodymium-based intermetallic compounds have been studied, which exhibited a variety of unusual ground states, such as antiferromagnetic nuclear ordering in $PrCu_2$,[11–13] antiferromagnetic quadrupolar ordering in $PrPb_3$,[14–16] heavy fermion behavior in $PrInAg_2$,[17] and Kondo behavior and antiferromagnetic ordering in $PrSn_3$.[18]

A new group of Pr compounds, PrMIn$_5$ (with M=Co, Rh, and Ir), was recently synthesized by Hieu *et al.*[19] These Pr-based 115 compounds crystallize in the $HoCoGa_5$ crystal structure, in which also the fascinating HF superconducting Ce-115 compounds, CeMIn$_5$ (with M=Co, Rh, and Ir), crystallize.[20] The Ce-115 HF superconductors display an extremely rich behavior of anomalous phenomena. $CeCoIn_5$ and $CeIrIn_5$ are superconductors at ambient pressure,[21,22] with T_c=2.3 and 0.4 K, respectively, whereas $CeRhIn_5$ becomes a superconductor (with T_c=2.1 K) under pressure.[23] At ambient pressure, $CeRhIn_5$ orders antiferromagnetically with an incommensurate spin spiral below the Néel temperature T_N=3.9 K.[24] Various experiments unambiguously established that the superconductivity is unconventional.[25–28] The occurrence of unconventional superconductivity in these materials appears to be closely connected to antiferromagnetic spin fluctuations (see, e.g., Refs. 29 and 30) for which reason the Ce-115's are considered as archetypal heavy fermion superconductors.

The recently synthesized PrMIn$_5$ (M=Co, Rh, and Ir) compounds[19] crystallize in the same $HoCoGa_5$ structure as the Ce-115 HF superconductors. The Pr-115 compounds reveal, however, a relatively low specific heat of $7-11$ mJ/mol K^2 and no magnetic ordering (down to 2 K), while the magnetic susceptibility is highly anisotropic, suggesting a ($4f^2$) singlet ground state in a tetragonal crystal field.[19] Also, Hieu *et al.*[19] reported measurements of the de Haas–van Alphen effect in the PrMIn$_5$ compounds. They concluded, from a comparison to measured and calculated results for the non-4f reference compound $LaRhIn_5$,[31] that the Fermi surface topology is approximately cylindrical. These findings suggest that the Pr 4f electrons in the Pr-115 compounds are localized. As an alternative, the itinerant 4f approach was recently applied to $PrCoIn_5$.[33]

de Haas–van Alphen (dHvA) measurements in connection with density functional theory (DFT) band-structure calculations are, in the first place, a very useful tool to analyze a multiband situation with a complicated Fermi surface and, in the second place, can give insight in the localization behavior of the 4f electrons. Recently, such investigations were carried out for the CeMIn$_5$ (M=Co, Rh, and Ir) compounds.[29,31,33] A characteristic feature in all three compounds is a substantial degree of a quasi-two-dimensional electronic structure; yet, there exist pertinent differences in the dHvA quantities of $CeCoIn_5$ and $CeIrIn_5$, on the one hand, and $CeRhIn_5$, on the other hand.[29] DFT calculations of the dHvA frequencies showed that when one treats the 4f electrons like itinerant states for $CeCoIn_5$ and $CeIrIn_5$, one can obtain a good agreement with the experimental dHvA frequencies, while for $CeRhIn_5$, the better agreement is obtained when the Ce 4f electron is treated as localized.[33,34]

Here, we report the DFT electronic structure investigation of the Pr-115 compounds. Specifically, we performed full-potential relativistic band-structure calculations for all three

compounds $PrCoIn_5$, $PrRhIn_5$, and $PrIrIn_5$. From these, we calculated the extremal Fermi surface cross sections and effective masses, and, in order to compare to the quantities investigated in the experiments,[19] we concentrate on the $H\|c$ case as well as on the angular dependence of the dHvA quantities. To investigate the localization behavior of the Pr $4f$ electrons, we performed calculations both by treating the $4f$ states either as delocalized valence states or as localized states, using the so-called open-core approach (see, e.g., Ref. 35 for a review).

After presenting our computational method (Sec. II) and a short discussion of the resulting band structures (Sec. III A), we describe the extremal orbits in Sec. III B. The critical comparison with experimental results (Sec. IV) allows us to draw conclusions concerning the electronic structures of the Pr-115 compounds in Sec. V.

II. COMPUTATIONAL APPROACH

We performed band-structure calculations using the fully relativistic version of the full-potential local orbital (FPLO) minimum-basis band-structure method,[36] RFPLO.[37] In our calculations, the following basis sets were adopted: for Co, Rh, Ir, and In, we used $3s3p3d$; $4s4p$, $4s4p4d$; $5s5p$, $5s5p5d$; $6s6p$, and $4s4p4d$; $5s5p$, respectively. The $5s5p$; $6s6p5d$ states of Pr are treated as valence states, while the $4f$ states of Pr have either been included as valence states or treated as core states. In the latter f-core approach, two nonspin-polarized Pr f electrons are treated as well localized core states without hybridization with valence states and give rise to a spherically averaged $4f$ charge density. No other f orbitals are included in the set of valence states; therefore, there are no unoccupied $4f$ states in this approach. The FPLO compression parameters x_0, which determine the radial extent of the basis orbitals, were optimized for each basis orbital separately by minimizing the total energy. For the site-centered potentials and densities, we used expansions in spherical harmonics up to $l_{max}=12$. The number of k points in the irreducible part of Brillouin zone was 196. The Perdew–Wang[38] parametrization of the exchange-correlation potential in the local density approximation (LDA) was used.

III. RESULTS

A. Calculated electronic structures

The compounds $PrMIn_5$ (M=Co, Rh, and Ir) crystallize in the tetragonal $HoCoGa_5$ structure, space group $P4/mmm$ (Space Group No. 123). This structure is built of alternating groups of $PrIn_3$ and MIn_2 stacked along the c axis. In our calculations, we adopted the recently published experimental lattice parameters: $a=4.600$ Å, $c=7.531$ Å, and $z(\mathrm{In})=0.3089$ ($PrCoIn_5$), $a=4.642$ Å, $c=7.521$ Å, and $z(\mathrm{In})=0.3052$ ($PrRhIn_5$), and $a=4.658$ Å, $c=7.510$ Å, and $z(\mathrm{In})=0.3047$ ($PrIrIn_5$).[19] The parameters used for $LaRhIn_5$ are $a=4.677$ Å, $c=7.599$ Å, and $z(\mathrm{In})=0.3078$.[31] The calculated band structures of $PrRhIn_5$ and $LaRhIn_5$ are presented in Figs. 1 and 2, respectively. As we shall see later on in more detail, the $4f$-core approach is the applicable description for all three Pr-115 compounds. Therefore, the energy bands

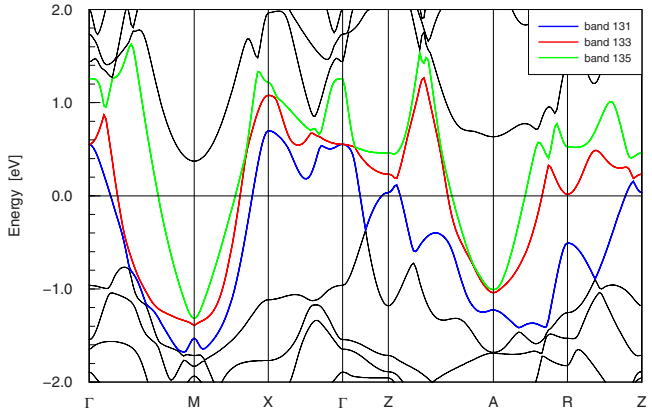

FIG. 1. (Color online) The calculated energy bands of $PrRhIn_5$, with the $4f$ states treated as core states. The bands crossing the Fermi energy are highlighted through their color.

shown in Fig. 1 for $PrRhIn_5$ have been obtained with the $4f$-core approach. The band structures of $PrCoIn_5$ and $PrIrIn_5$ are only slightly different from the one of $PrRhIn_5$ and therefore not presented here. We find for all three Pr-115 compounds and for $LaRhIn_5$ three bands which cross the Fermi energy. These bands are denoted as band 131, band 133, and band 135, according to their number in the valence band complex of the fully relativistic calculation, counted from below (note that the bands are twofold Kramers degenerate).

Comparing in more detail the energy bands depicted in Figs. 1 and 2, we first note that the two band structures in the vicinity of E_F are very similar along the high-symmetry lines Γ-M-X. The crossing points of bands 131, 133, and 135 (in identical order) with the Fermi level are clearly visible. Along other high-symmetry lines, there exist several differences in the energy bands of $PrRhIn_5$ and $LaRhIn_5$. For example, the Fermi level crossings of band 131 close to the Z point differ and band 133 does not cross the Fermi level at R. Also, there exists a difference in the Fermi level crossings of band 131 along the R-Z line, close to the Z point. As a consequence, the Fermi surfaces and dHvA effect are expected to be different: the $PrMIn_5$ compounds have a smaller number of extremal orbits than $LaRhIn_5$ for $H\|c$. By calcu-

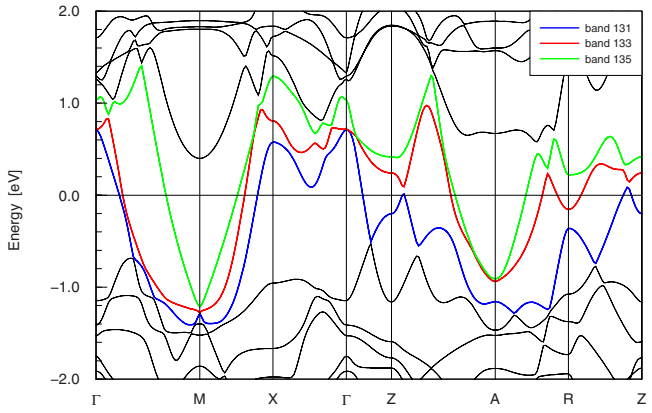

FIG. 2. (Color online) The calculated energy bands of $LaRhIn_5$, the non-f-electron reference compound.

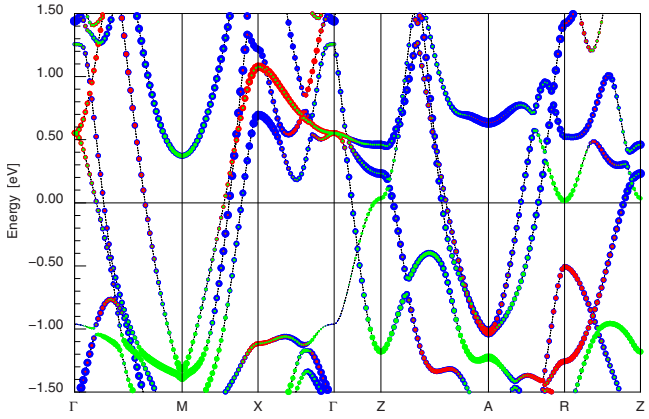

FIG. 3. (Color online) The calculated (4*f* core) energy bands of nonmagnetic $PrRhIn_5$ in the vicinity of the Fermi level. The amounts of In 5*p*, Pr 5*d*, and Rh 4*d* characters are indicated by the colors and fatness of the bands; green symbols denote Rh 4*d*, red Pr 5*d*, and blue In 5*p*, respectively.

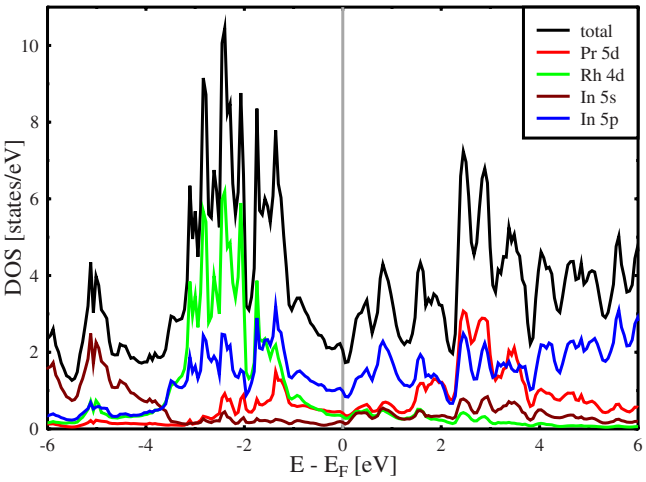

FIG. 4. (Color online) Total and partial DOSs of nonmagnetic $PrRhIn_5$, calculated with the 4*f*-core approach.

lating additionally the different band weights, shown in Fig. 3, we see that the bands which cross the Fermi level in Fig. 1 have a considerable Rh 4*d* (green), Pr 5*d* (red), and In 5*p* (blue) character. Most pronounced is the In 5*p* character (band crossing E_F near the *Z* point, between *A* and *R* and *M* and *X*) and the Rh 4*d* character (green symbols at the *R* point and close to the *Z* point). If we compare Figs. 1 and 2 between the *M* and Γ points or between *M* and *X*, we find in both cases three bands crossing the Fermi energy. The two upper bands (133 and 135) give rise to closed orbits centered at *M* (see Fig. 5), which are of predominantly In 5*p* character and present for all Pr-115 compounds. The same is true for the two electronlike bands centered around the *A* point. From computed band weights for $LaRhIn_5$ (not shown), we can trace back these differences between $LaRhIn_5$ and $PrRhIn_5$ to small energy differences in some of the band states. The Rh 4*d* derived states at *R* and *Z* (cf. green symbols in Fig. 3) are placed at a somewhat deeper energy for La $RhIn_5$. The Pr 5*d* states (red symbols in Fig. 3) are conversely higher in energy for $PrRhIn_5$ than the corresponding La 5*d* states in $LaRhIn_5$. In Fig. 4, we show the calculated total and partial densities of states (DOSs) of nonmagnetic $PrRhIn_5$. The partial DOS is rather similar to that of the $LaRhIn_5$ compound. The dominant contribution to the total DOS in the vicinity of E_F stems from the In 5*p* states, as well as the Pr 5*d* and Rh 4*d* states. A small contribution from In 5*s* states exists, too.

B. Fermi surface and extremal orbits

The extremal orbits for $H \| c$ and the angular dependence of the theoretical dHvA frequencies have been calculated using the numerical schemes discussed in Refs. 39 and 40. In order to visualize the existing extremal orbits, we show in Fig. 5 the computed Fermi surface of nonmagnetic $PrRhIn_5$ and $LaRhIn_5$. The Fermi surface sheets shown correspond, from top to bottom, to bands 131, 133, and 135. To label the extremal orbits, we use the same notation as in previous experimental investigations,[19,31] with the following additions: we label orbit α_2, which was found in experiment for all Pr-115 and for $LaRhIn_5$ compounds, and orbit β_3, which arises from the same Fermi surface sheet as β_1 and β_2. The main experimental extremal orbits are denoted[19,31] α_i ($i=1,2,3$) and β_i ($i=1,2,3$), which are located on the two tubular Fermi surface sheets corresponding to bands 133 and 135, respectively. Due to the corrugation of these sheets along the *M*-*A* axis, there exist three distinct extremal orbits along the *z* direction; orbits β_3 and α_1 occur for $k_z=0.24$ and $k_z=0.18$, respectively. The other extremal orbits, ε_1 and a_i (with $i=1,2,3$) are located on the more three-dimensional

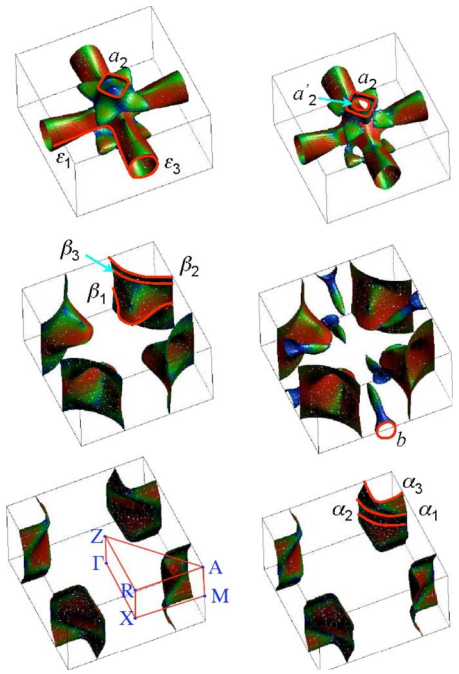

FIG. 5. (Color online) Calculated Fermi surface of nonmagnetic $PrRhIn_5$ (left-hand panels) and $LaRhIn_5$ (right-hand panels), with extremal orbits indicated. The Fermi surface sheets correspond, from top to bottom, to bands 131, 133, and 135.

TABLE I. Comparison of experimental (Ref. 19) and calculated dHvA frequencies F (in kT) and the cyclotron masses m (in electron masses m_0) for $PrCoIn_5$ with $H\|c$.

Orbit	Central point	Band No.	F (kT)		$\|m\|$ (m_0)	
			Calc.	Expt.	Calc.	Expt.
ε_1	M	131	13.40		0.98	
β_1	M	133	10.32	9.93	0.70	1.66
β_2	A	133	5.96	5.97	0.71	0.76
β_3	$A'_{k_z=0.24}$	133	5.53		0.79	
α_1	$A'_{k_z=0.18}$	135	4.73	4.65	0.69	0.70
α_2	M	135	3.99	3.97	0.49	0.83
α_3	A	135	4.00		0.61	
a_2	Z	131	0.74	0.73	0.26	0.30

Fermi surface sheets of band 131. The three a_i orbits are located near the Z point and ε_1 is located in the $z=0$ plane. The latter orbit has a high frequency and a high cyclotron mass, and, due to its location, its observation could depend sensitively on the alignment of the crystallographic c axis and the magnetic field. So far, it could only be detected for $PrIrIn_5$.[19] The α and β orbits are experimentally the best visible ones.

In Tables I–III, we compare the calculated and experimental dHvA frequencies and cyclotron masses for $PrCoIn_5$, $PrRhIn_5$, and $PrIrIn_5$, respectively. In general, we observe from the Tables I–III a rather good agreement between theory and experiment, in particular, for orbits α_i $(i=1,2,3)$ and β_i $(i=1,2,3)$. The dHvA frequencies are well given by the present open-core calculations. The dHvA cyclotron masses do show deviations of the order of a factor of 2. However, taking into account the absence of many-body enhancement in our calculations, such a deviation is not unusual. For $PrIrIn_5$ (Table III), all experimentally observed extremal orbits correspond nicely to computed orbits. For this compound, also, the high frequency orbit ε_1 was experimentally detected, and its dHvA frequency corresponds very well to the computed result.

In the experimental investigation of Hieu *et al.*,[19] a comparison was made to calculated as well as experimental results for $LaRhIn_5$.[31] As we mentioned before, the computed Fermi surface of this non-$4f$ reference compound is very similar to that of the Pr-115's, but there are also some differences. In Table IV, we compare our present calculations for $LaRhIn_5$ with the full-potential linearized augmented plane waves (FLAPW) calculations as well as experimental results of Ref. 31. The agreement between the two theoretical data and between the theory and experiment is rather good. Due to the already mentioned different shapes of the Fermi surface sheet corresponding to band 133, the extremal orbit β_3 does not exist, neither in experiment nor in the calculations. Differences with regard to the Pr-115 compounds also exist in the Fermi surface part due to band 131 around Z. In our calculations for $LaRhIn_5$, we included the $4f$ states as delocalized valence states. Comparing in more detail the two sets of computed data, we note that the FLAPW method gives, for most of the extremal orbits, a somewhat larger dHvA frequency and mass, which is in better agreement with the experiment. This might be related to small differences in the used lattice parameters or the exchange-correlation functional. There is a good agreement of the theory with experimental results of Shishido *et al.*[31] (who give, however, not all frequencies that exist). Only the orbit around R of band 133 was apparently never observed. Band 131 now gives rise to two extremal orbits around Z, which we denote a_2 and a'_2. It seems that only the larger orbit a_2 was observed experimentally. The calculated cyclotron masses are for $LaRhIn_5$ closer to the measured values than is the case for the three Pr-115 compounds. This indicates that although the Pr $4f$ electrons are localized, they still play a small role in the many-body enhancement. Such enhancement could occur through Pr on-site f-d exchange interactions, which couple f spin fluctuations to Pr $5d$ states near the Fermi level. The measured[20] specific heat coefficients of the Pr-115 compounds are quite small, $\gamma=11$, 7.7, and 7.2 mJ/mol K^2, respectively, for $PrCoIn_5$, $PrRhIn_5$, and $PrIrIn_5$. These can be compared with our calculated unenhanced specific heat coefficients, which are, respectively, $\gamma=6.0$, 4.8, and 4.6 mJ/mol K^2. The many-body enhancement of nearly a factor of 2 in the specific heat coefficients is in accordance with the enhancement factor observed for the cyclotron masses (see Tables I–III).

TABLE II. Comparison of experimental (Ref. 19) and calculated dHvA-data of $PrRhIn_5$ for $H\|c$.

Orbit	Central point	Band No.	F (kT)		$\|m\|$ (m_0)	
			Calc.	Expt.	Calc.	Expt.
ε_1	M	131	12.42		0.82	
β_1	M	133	10.15	10.04	0.63	0.93
β_2	A	133	6.06	6.30	0.55	0.76
β_3	$A'_{k_z=0.24}$	133	5.96	6.12	0.59	0.65
α_1	$A'_{k_z=0.18}$	135	4.59	4.65	0.54	0.56
α_2	M	135	3.95	3.93	0.46	0.40
α_3	A	135	3.50	3.40	0.47	0.31
a_2	Z	131	0.51	0.39	0.23	0.60

TABLE III. As Table II, but for $PrIrIn_5$.

Orbit	Central point	Band No.	F (kT)		$\|m\|$ (m_0)	
			Calc.	Expt.	Calc.	Expt.
ε_1	M	131	13.66	13.84	0.93	1.72
β_1	M	133	10.02	9.82	0.65	1.20
β_2	A	133	5.61	5.90	0.64	1.41
β_3	$A'_{k_z=0.24}$	133	5.24	5.88	0.66	1.48
α_1	$A'_{k_z=0.18}$	135	4.16	4.21	0.53	0.92
α_2	M	135	3.80	3.76	0.48	0.77
α_3	A	135	3.32	3.26	0.45	0.79
a_2	Z	131	0.51	0.47	0.23	0.94

C. Angular dependence

For further comparison to the experiment, we investigated in addition the angular dependence of the dHvA frequencies

TABLE IV. Comparison of experimental (Ref. 31) and theoretical dHvA data of $LaRhIn_5$ for $H\|c$. The calculations of Ref. 31 were performed with the FLAPW method, the calculations denoted "present" by the FPLO method.

Orbit	Central point	Band No.	F (kT)			$\|m\|$ (m_0)		
			Present	Calc.[a]	Expt.	Present	Calc.[a]	Expt.
ε_1	M	131	12.31	12.46		0.94	1.14	
β_1	M	133	9.91	10.11	10.02	0.66	0.88	0.98
β_2	A	133	5.76	6.08	6.13	0.58	0.62	0.73
α_1	$A'_{k_z=0.18}$	135	4.26	4.33	4.62	0.57	0.63	0.69
α_2	M	135	3.45	3.56	3.76	0.48	0.53	0.51
α_3	A	135	3.30	3.12	3.56	0.49	0.55	0.64
b	R	133	0.37					
a_2	Z	131	0.63		0.60	0.37		
a'_2	Z	131	0.31					

[a]Reference 31.

of the branches for the three Pr-115 compounds (treating the $4f$ electrons as localized) and $LaRhIn_5$. A comparison of the computed and experimental results[19] is shown in Fig. 6. As can be seen, the characteristic angular dependence of the various dHvA branches is well reproduced.

The rather two-dimensional shapes of the Fermi surface sheets of bands 133 and 135 gives rise to the steep upturn observed for the α and β branches when the field is turned toward the [100] direction. The other extremal orbits, ε_1 and the a_2 orbits, behave differently: the large orbit ε_1 disappears

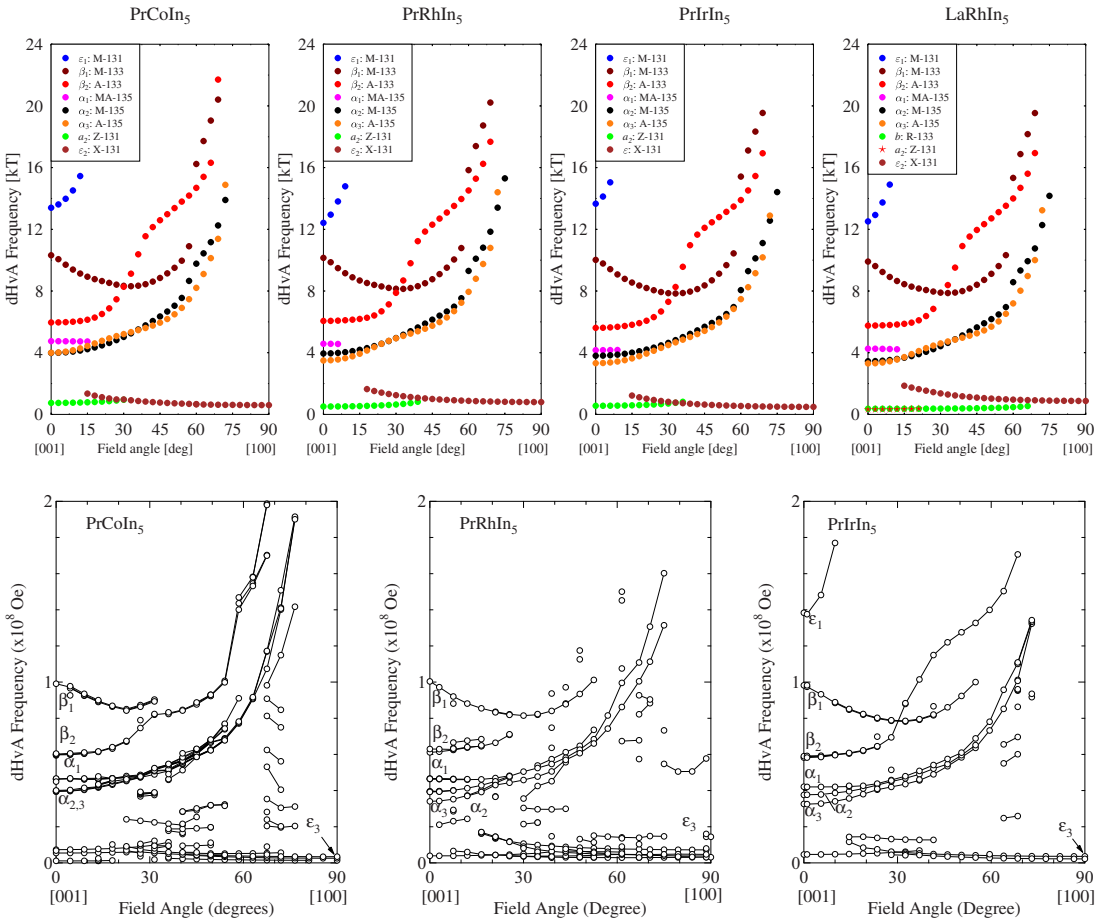

FIG. 6. (Color online) Top: The calculated angular dependence of the dHvA frequencies of $PrMIn_5$ (M=Co, Rh, and Ir) and of $LaRhIn_5$. Bottom: measured angular dependence of the main dHvA frequencies of the Pr-115 compounds (Ref. 41), after Hieu *et al.* (Ref. 19).

TABLE V. Theoretical dHvA frequencies for $H \| a$.

Orbit	Central point	Band No.	F (kT)			
			$PrCoIn_5$	$PrRhIn_5$	$PrIrIn_5$	$LaRhIn_5$
ε_2	X	131	0.603	0.799	0.488	0.872
ε_3'	$X'_{k_z=0.10}$	131	0.329	0.463	0.410	0.492
ε_3''	$X'_{k_z=0.23}$	131	0.331	0.333	0.174	0.232

when the field is turned away from the c axis, while the orbit a_2 increases slightly when the field is rotated, but then it disappears. When the field is approximately along the [100] axis, there exists another Fermi surface part (the tubular arms of the Fermi surface sheet of band 131, see Fig. 5), which gives rise to three extremal dHvA orbits. The corresponding dHvA orbits are denoted as ε_2, ε_3', and ε_3'', and their calculated frequencies are shown in Table V.

IV. SUMMARY AND CONCLUSIONS

In recent years, praseodymium-based crystals have entered the scientific focus because of observed anomalous phenomena that are related to the Pr $4f$ electrons. Here, we have investigated the Pr-115 compounds, which crystallize in the same tetragonal $HoCoGa_5$ structure as the family of Ce-115 unconventional superconductors. The behavior of the Pr $4f$ electrons is, however, significantly different from that of the Ce $4f$ electrons in the isostructural analogs. Our investigation confirms that the Pr $4f$ electrons are basically localized in the Pr-115 crystals. This is most clearly demonstrated by the good agreement between experimental and calculated angular dHvA quantities, which we achieve when the Pr $4f$ states are treated as core states. In another recent computational investigation,[32] the Pr $4f$ electrons were adopted to be delocalized, but the here achieved correspondence between the computed and measured dHvA data does support the localized view point. We checked this statement by additional calculations with $4f$ states included in the valence basis (not reported here). Also, as pointed out by Hieu *et al.*,[19] the correspondence between the measured dHvA quantities of the Pr-115 compounds and $LaRhIn_5$ shows that there are essentially no Pr $4f$ states present at the Fermi energy. Our calculations for $LaRhIn_5$ confirm this point: the Fermi surface of $LaRhIn_5$ is similar to that of the Pr-115 compounds when the Pr $4f$ states are treated as core states. There exist, nevertheless, several differences between the Fermi surfaces of the La- and Pr-based 115 compounds. These differences could yet be more clearly discerned in careful dHvA studies on high-quality single crystals, something which would complete our understanding of these materials.

LDA calculations, in which f electrons are treated as valence states, can lead to a poor description of the physical properties of lanthanide materials because of the occurrence of an unphysical broad $4f$ resonance near the Fermi energy. The presented $4f$-core calculations for the Pr-115 compounds provide Fermi surfaces which are in good quantitative agreement with experiment: the computed dHvA frequencies compare closely with the experimental data. The computed dHvA cyclotron masses follow the same trends as the measured masses, but the latter are larger due to many-body enhancement factors. Two small differences between theory and experiment exist in the number of observed branches. Our calculations predict the presence of the ε_1 dHvA branch for all three Pr-115 compounds. So far, this branch could be observed experimentally for $PrIrIn_5$ only, but it might well be present for all three compounds. Theory also predicts three a_i branches for the Pr-115 materials, of which, so far, only the a_2 branch—which has the largest dHvA frequency—appears to be unambiguously detected.

Lastly, we propose that pressure experiments on Pr-115 crystals might provide interesting information. Detailed dHvA experiments under pressure on $CeRhIn_5$ revealed,[30] recently, a crossover from antiferromagnetic localized $4f$ behavior to a heavy fermion superconducting state in which the $4f$ electron partially delocalizes. A similar behavior might occur for the Pr-115 materials, albeit presumably at a higher pressure.

ACKNOWLEDGMENTS

We thank Dai Aoki and the authors of Ref. 19 for providing us with the experimental angular dependent dHvA data for the Pr-115 compounds. This work was supported by the Swedish VR and SNIC and by the Deutsche Forschungsgemeinschaft, SFB 463/B11.

*Present address: Department of Physics, Uppsala University, Box 530, S-751 21 Uppsala, Sweden.

[1] Z. Fisk, H. R. Ott, T. M. Rice, and J. L. Smith, Nature (London) **320**, 124 (1986).

[2] Z. Fisk, D. W. Hess, C. J. Pethick, D. Pines, J. L. Smith, J. D. Thompson, and J. O. Willis, Science **239**, 33 (1988).

[3] N. Grewe and F. Steglich, in *Handbook of the Physics and Chemistry of Rare Earths*, edited by K. A. Gschneidner, Jr. and L. Eyring (Elsevier, Amsterdam, 1991), Vol. 14, p. 343.

[4] E. D. Bauer, N. A. Frederick, P.-C. Ho, V. S. Zapf, and M. B. Maple, Phys. Rev. B **65**, 100506(R) (2002).

[5] H. Sugawara, T. D. Matsuda, K. Abe, Y. Aoki, H. Sato, S. Nojiri, Y. Inada, R. Settai, and Y. Ōnuki, Phys. Rev. B **66**, 134411 (2002).

[6] D. E. MacLaughlin, J. E. Sonier, R. H. Heffner, O. O. Bernal, B.-L. Young, M. S. Rose, G. D. Morris, E. D. Bauer, T. D. Do, and M. B. Maple, Phys. Rev. Lett. **89**, 157001 (2002).

[7] H. Kotegawa, M. Yogi, Y. Imamura, Y. Kawasaki, G.-q. Zheng, Y. Kitaoka, S. Ohsaki, H. Sugawara, Y. Aoki, and H. Sato, Phys. Rev. Lett. **90**, 027001 (2003).

[8] Y. Aoki, A. Tsuchiya, T. Kanayama, S. R. Saha, H. Sugawara, H. Sato, W. Higemoto, A. Koda, K. Ohishi, K. Nishiyama, and R.

Kadono, Phys. Rev. Lett. **91**, 067003 (2003).
[9] G. Seyfarth, J. P. Brison, M.-A. Méasson, J. Flouquet, K. Izawa, Y. Matsuda, H. Sugawara, and H. Sato, Phys. Rev. Lett. **95**, 107004 (2005).
[10] K. Kuwahara, K. Iwasa, M. Kohgi, K. Kaneko, N. Metoki, S. Raymond, M.-A. Méasson, J. Flouquet, H. Sugawara, Y. Aoki, and H. Sato, Phys. Rev. Lett. **95**, 107003 (2005).
[11] K. Andres, E. Bucher, J. P. Maita, and S. A. Cooper, Phys. Rev. Lett. **28**, 1652 (1972).
[12] R. Settai, S. Araki, P. Ahmet, M. Abliz, K. Sugiyama, Y. Ōnuki, T. Goto, H. Mitamura, T. Goto, and S. Takayanagi, J. Phys. Soc. Jpn. **67**, 636 (1998).
[13] A. Schenck, F. N. Gygax, and Y. Ōnuki, Phys. Rev. B **68**, 104422 (2003).
[14] D. Aoki, Y. Katayama, R. Settai, Y. Inada, Y. Ōnuki, H. Harima, and Z. Kletowski, J. Phys. Soc. Jpn. **66**, 3988 (1997).
[15] T. Tayama, T. Sakakibara, K. Kitami, M. Yokoyama, K. Tenya, H. Amitsuka, D. Aoki, Y. Ōnuki, and Z. Kletowski, J. Phys. Soc. Jpn. **70**, 248 (2001).
[16] T. Onimaru, T. Sakakibara, N. Aso, H. Yoshizawa, H. S. Suzuki, and T. Takeuchi, Phys. Rev. Lett. **94**, 197201 (2005).
[17] A. Yatskar, W. P. Beyermann, R. Movshovich, and P. C. Canfield, Phys. Rev. Lett. **77**, 3637 (1996).
[18] R. Settai, K. Sugiyama, A. Yamaguchi, S. Araki, K. Miyake, T. Takeuchi, K. Kindo, Y. Ōnuki, and Z. Kletowski, J. Phys. Soc. Jpn. **69**, 3983 (2000).
[19] N. V. Hieu, H. Shishido, A. Thamizhavel, R. Settai, S. Araki, Y. Nozue, T. Matsuda, Y. Haga, T. Takeuchi, H. Harima, and Y. Ōnuki, J. Phys. Soc. Jpn. **74**, 3320 (2005).
[20] E. G. Moshopoulou, J. L. Sarrao, P. G. Pagliuso, N. O. Moreno, J. D. Thompson, Z. Fisk, and R. M. Ibberson, Appl. Phys. A: Mater. Sci. Process. **74**, S895 (2002).
[21] C. Petrovic, R. Movshovich, M. Jaime, P. G. Pagliuso, M. F. Hundley, J. L. Sarrao, Z. Fisk, and J. D. Thompson, Europhys. Lett. **53**, 354 (2001).
[22] C. Petrovic, P. G. Pagliuso, M. F. Hundley, R. Movshovich, J. L. Sarrao, J. D. Thompson, Z. Fisk, and P. Monthoux, J. Phys.: Condens. Matter **13**, L337 (2001).
[23] H. Hegger, C. Petrovic, E. G. Moshopoulou, M. F. Hundley, J. L. Sarrao, Z. Fisk, and J. D. Thompson, Phys. Rev. Lett. **84**, 4986 (2000).
[24] Wei Bao, P. G. Pagliuso, J. L. Sarrao, J. D. Thompson, Z. Fisk, J. W. Lynn, and R. W. Erwin, Phys. Rev. B **62**, R14621 (2000).
[25] G.-q. Zheng, K. Tanabe, T. Mito, S. Kawasaki, Y. Kitaoka, D. Aoki, Y. Haga, and Y. Ōnuki, Phys. Rev. Lett. **86**, 4664 (2001).
[26] K. Izawa, H. Yamaguchi, Y. Matsuda, H. Shishido, R. Settai, and Y. Ōnuki, Phys. Rev. Lett. **87**, 057002 (2001).
[27] R. Movshovich, M. Jaime, J. D. Thompson, C. Petrovic, Z. Fisk, P. G. Pagliuso, and J. L. Sarrao, Phys. Rev. Lett. **86**, 5152 (2001).
[28] R. J. Ormeno, A. Sibley, C. E. Gough, S. Sebastian, and I. R. Fisher, Phys. Rev. Lett. **88**, 047005 (2002).
[29] H. Shishido, R. Settai, H. Harima, and Y. Ōnuki, J. Phys. Soc. Jpn. **74**, 1103 (2005).
[30] L. D. Pham, T. Park, S. Maquilon, J. D. Thompson, and Z. Fisk, Phys. Rev. Lett. **97**, 056404 (2006).
[31] H. Shishido, R. Settai, D. Aoki, S. Ikeda, H. Nakawaki, N. Nakamura, T. Iizuka, Y. Inada, K. Sugiyama, T. Takeuchi, K. Kindo, T. C. Kobayasi, Y. Haga, H. Harima, Y. Aoki, T. Namiki, H. Sato, and Y. Ōnuki, J. Phys. Soc. Jpn. **71**, 162 (2002).
[32] T. Maehira and T. Hotta, J. Phys. Soc. Jpn. **75**, S262 (2006).
[33] S. Elgazzar, I. Opahle, R. Hayn, and P. M. Oppeneer, Phys. Rev. B **69**, 214510 (2004).
[34] S. Elgazzar, I. Opahle, R. Hayn, and P. M. Oppeneer, J. Magn. Magn. Mater. **290-291**, 388 (2005).
[35] M. Richter, J. Phys. D **31**, 1017 (1998).
[36] K. Koepernik and H. Eschrig, Phys. Rev. B **59**, 1743 (1999); http:\\www.fplo.de\
[37] H. Eschrig, M. Richter, and I. Opahle, in *Relativistic Electronic Structure Theory: Applications*, edited by P. Schwerdtfeger (Elsevier, Amsterdam, 2004), Pt. II, pp. 723–776.
[38] J. P. Perdew and Y. Wang, Phys. Rev. B **45**, 13244 (1992).
[39] P. M. Oppeneer and A. Lodder, J. Phys. F: Met. Phys. **17**, 1901 (1987).
[40] I. Opahle (unpublished); see also S. Elgazzar, Ph.D. thesis, TU Dresden, 2005.
[41] Reproduced with permission of the Journal of the Physical Society of Japan.